Published in final edited form as:

Stem Cells. 2009 February ; 27(2): 280–289. doi:10.1634/stemcells.2008-0842.

Gliotypic Neural Stem Cells Transiently Adopt Tumorigenic Properties During Normal Differentiation

Noah M. Walton[a,b], **Gregory E. Snyder**[b], **Donghyun Park**[b], **Firas Kobeissy**[a], **Bjorn Scheffler**[a,c], and **Dennis A. Steindler**[a]

[a]Department of Neuroscience, McKnight Brain Institute, University of Florida, Gainesville, Florida, USA

[b]Department of Human Genetics, University of Chicago, Chicago, Illinois, USA

[c]Institute for Reconstructive Neurobiology, LIFE and Brain, University of Bonn, Bonn, Germany

Abstract

An increasing body of evidence suggests that astrocytic gliomas of the central nervous system may be derived from gliotypic neural stem cells. To date, the study of these tumors, particularly the identification of originating cellular population(s), has been frustrated by technical difficulties in accessing the native niche of stem cells. To identify any hallmark signs of cancer in neural stem cells or their progeny, we cultured subventricular zone-derived tissue in a unique in vitro model that temporally and phenotypically recapitulates adult neurogenesis. Contrary to some reports, we found undifferentiated neural stem cells possess few characteristics, suggesting prototumorigenic potential. However, when induced to differentiate, neural stem cells give rise to intermediate progenitors that transiently exhibit multiple glioma characteristics, including aneuploidy, loss of growth-contact inhibition, alterations in cell cycle, and growth factor insensitivity. Further examination of progenitor populations revealed a subset of cells defined by the aberrant expression of (the pathological glioma marker) class III β-tubulin that exhibit intrinsic parental properties of gliomas, including multilineage differentiation and continued proliferation in the absence of a complex cellular regulatory environment. As tumorigenic characteristics in progenitor cells normally disappear with the generation of mature progeny, this suggests that developmentally intermediate progenitor cells, rather than neural stem cells, may be the origin of so-called “stem cell-derived” tumors.

Correspondence: Dennis A. Steindler, Ph.D., McKnight Brain Institute, Program in Stem Cell Biology and Regenerative Medicine, University of Florida, 100 South Newell Drive, Gainesville, Florida 32610, USA. Telephone: 352-273-8500; Fax: 352-846-0185; steindler@mbi.ufl.edu.

Author contributions: N.M.W.: conception and design, collection and assembly of data, data analysis, manuscript writing, final approval of manuscript; G.E.S. and D.P.: conception and design, data analysis; F.K.: collection of data; B.S.: conception and design; D.A.S.: design of thesis experiments of the first author, financial support, manuscript writing.

Disclosure of Potential Conflicts of Interest

The authors indicate no potential conflicts of interest.

See www.StemCells.com for supporting information available online.

Keywords

Neurogenesis; Glioblastoma; Hyperplasia; Progenitor; Stem cell

Introduction

Increasing evidence suggests that tumors of the nervous system are derived from proliferatively active neural stem cells (NSCs) residing in defined neuropoietic niches of the adult brain. This evidence is manifold and includes the identification of neural stem cell markers [1] and the isolation of neurosphere-forming cells in brain tumor specimens [2–6]. These “stem cell tumors” are widely believed to originate from relatively few tumor-initiating cells, likely arising from a disruption in the regulatory mechanisms governing self-renewal [7, 8]. In particular, the subventricular zone (SVZ) is regarded as the most likely source for gliomas [6, 7, 9, 10], highly malignant tumors of the mature central nervous system (CNS).

In adults, subventricular NSCs exist as a population of relatively quiescent astrotypic cells that persist throughout life [11]. These cells generate committed progeny via asymmetric divisions that produce transit-amplifying progenitor cells that further divide to yield mature neuroblasts [12, 13]. Although it remains unclear whether NSCs and/or their intermediate progenitors form the tumor-originating population for such tumors [6, 14], a growing number of observations suggest that progenitor cells may compose the primary originating population. First, NSCs of the SVZ divide infrequently, whereas intermediate progenitors are believed to possess more rapid cell cycling times [15, 16]. As the generation of a cancerous phenotype has been predicted to arise from a relatively small number of independent mutations [17], it is likely that NSCs, which exist throughout life [11], accumulate mutations that may result in transformed progeny. Both progenitors and tumor cells retain common traits from parental populations [18], providing for the possibility that progenitor cells may be capable of providing the degree of multipotency to produce the variegated cell types observed in astrocytic gliomas.

A number of hallmark characteristics are associated with astrocytic tumors of the CNS, including insensitivity to mitogenic factors, aneuploidy, dysregulation of cell cycle machinery, hyperplasia, multilineage capacity, expression of aberrant markers (particularly class III β-tubulin), and (in cultured tumors) failure to enter into anoikis and failure of growth-contact inhibition [17]. These traits, to some degree, are believed to be shared by the tumor-originating population. However, in vivo studies of NSCs and their respective contributions to tumorigenesis are hampered by the relative inaccessibility of the neuropoietic niche. To more thoroughly examine NSCs and their progeny in a tumorigenic context, we studied naïve and differentiating subventricular NSCs using an in vitro model that phenotypically and temporally recapitulates in vivo neurogenesis [19]. Using this model, we induced the synchronous differentiation of subventricular NSCs into mature neurons and compared cells from developmental states enriched for astrotypic NSCs, their intermediate progenitor cells, and newly generated neuroblasts for established cancerous phenotypes. Interestingly, progenitor cells most frequently exhibit glioma traits, suggesting

they more closely resemble potential originating cells than any cell in the developmental continuum.

Although progenitor cells natively express many similar characteristics of tumor-forming cells, these traits are transient, routinely disappearing with the appearance of mature progeny. However, when maintained in isolation, progenitor cells retain sustained proliferative indices and multilineage potential, suggesting that intrinsic determination and/or regulation from non-neurogenic cells is, to some extent, involved in normal neurogenesis. This is supported by an increase in cell cycle checkpoint gene expression following differentiation, suggesting regulatory arrest or apoptosis as progenitor cells continue to generate progeny.

Directed examination of progenitor cells reveals many of the characteristic proliferative traits for progenitors. In tumors of glial origin, class III β-tubulin is atypically expressed in a differentiation-independent fashion [20, 21]. It is thus possible that class III β-tubulin is a relevant marker of tumorigenicity; most notably, an aberrant expression of βIII tubulin has been reported in astrocytoma, neurocytoma, dysembryoplastic neuroepithelial tumors, subependymal giant cell astrocytoma, neuroblastoma, neuroendocrine lung tumors, giant cell glioblastoma, pleomorphic xanthoastrocytoma, ependymoma, ganglioglioma, and breast tumors [20 –30]. As such, non-neuronal expression of class III β-tubulin in normal tissues may have significant predictive value for identifying and characterizing progenitors and/or protogliomal cells. Indeed, class III β-tubulin$^+$ progenitors exhibited the majority of cell division, suggesting that they contribute directly to the tumorigenic features in heterologous cultures. Taken together, these findings suggest a prominent role of intermediate progenitors as naturally occurring proto-oncogenic cells.

Materials and Methods

Isolation and Derivation of Neural Stem Cells

Whole-ventricular tissue dissociates were prepared as previously described [19]. Briefly, primary tissue was gathered and pooled from 8-day-old C57/B6 mice (n = 6) and mice expressing enhanced green fluorescent protein under the control of the nestin promoter (n = 4; gift from Dr. Grigori Enikolopov). Animals were deeply anesthetized with avertin and decapitated, and their brains removed. Lateral periventricular tissue was microdissected and manually dissociated into 1-mm^3 pieces under sterile conditions in 1× phosphate-buffered saline (PBS; 25°C, pH 7.3) lacking $CaCl_2$ or $MgCl_2$. Primary tissue was removed and stored overnight in ice-cold Dulbecco's modified Eagle's medium with Ham's F-12 medium supplements (DMEM/F-12; Gibco, Grand Island, NY, http://www.invitrogen.com) containing antibiotics (20 mg/ml penicillin, 20 mg/ml streptomycin, and 25 ng/ml amphotericin B; Sigma-Aldrich, St. Louis, http://www.sigmaaldrich.com). Dissociates were collected by centrifugation (4,000g, 5 minutes) and resuspended in 0.25% trypsin (10^6 cells per ml, 15 minutes, 37°C, pH 7.3; Sigma-Aldrich). Dissociates were further triturated using restricted-bore pipetting. Cells were collected by centrifugation (4,000g, 5 minutes), resuspended in proliferative medium (10^6 cells per ml), and seeded onto uncoated 75-cm^2 culture flasks (Invitrogen, Carlsbad, CA, http://www.invitrogen.com) overnight (12 hours, 37°C, 5% humidified CO_2). Unattached cells were subsequently collected and plated onto

uncoated 60-mm plastic dishes (Corning Costar, Corning, NY, http://www.corning.com/lifesciences) in defined proliferative medium at a density of 2×10^4 cells per cm^2. Proliferative medium was composed of DMEM/F-12 containing N2 supplements, 35 μg/ml bovine pituitary extract (Sigma-Aldrich), 1× antibiotics, 5% fetal calf serum (FCS; HyClone, Logan, UT, http://www.hyclone.com), and 40 ng/ml epidermal growth factor (EGF) and basic fibroblast growth factor (bFGF; R&D Systems Inc., Minneapolis, http://www.rndsystems.com). Twenty nanograms of EGF and bFGF was supplemented every 2 days to prevent differentiation, although maintenance of undifferentiated state was maintained with as little as 10 ng/ml of each mitogen administered every 4th day. Cells were frozen in aliquots of 1 million cells in DMEM/F-12 containing 10% FCS and 20% dimethyl sulfoxide (vol/vol; Sigma-Aldrich). Cells were proliferated to 90%–95% visual confluence, washed with 1× PBS, and dissociated with 0.25% trypsin (37°C, 5 minutes). Passaged cells were counted using trypan dye exclusion as primary viability criteria and were replated at a density of 2×10^4 cells per cm^2 onto uncoated 60-mm plastic dishes (Corning Costar). Significance ($p < .05$) was calculated using a Student's *t* test and one-way analysis of variance (ANOVA). In vitro images of cultured cells were captured using a Nikon Eclipse TS-100 bright-field microscope (Nikon, Tokyo, http://www.nikon.com) and a Spot 3.1 digital camera (Diagnostic Instruments, Sterling Heights, MI, http://www.diaginc.com).

Differentiation of Adherent Subventricular Dissociates

Passage 3 dissociates from postnatal day 8 age-matched animals were plated onto glass coverslips coated with laminin and polyornithine (LPO) or poly-L-lysine in proliferative medium at a density of 2×10^4 cells per cm^2. To induce differentiation, proliferative medium was removed and replaced with medium lacking serum, bFGF, and EGF. 5′-Bromodeoxyuridine (BrDU) incorporation in differentiating cultures was assessed using pulsed additions of 10 μM BrDU to culture medium in 24-hour periods, beginning 24 hours prior to induction of differentiation and proceeding until 96 hours following induction of differentiation. To isolate cells at various stages of differentiation, triplicate coverslips were analyzed for each experiment. Cells were analyzed during proliferation and every 12–96 hours of total differentiation. For clonal analysis, cells were randomly selected from trypsinized passage 3 SVZ proliferating monolayers and monolayers induced to differentiate for 1 and 4 days. Clones were plated and maintained in medium lacking serum and growth factors for 3 days, and they were evaluated for cell number and immunophenotype. A minimum of 500 clones were examined for each condition.

Semiquantitative Polymerase Chain Reaction

Semiquantitative polymerase chain reaction (PCR) was performed on a range of selected genes (supporting information Fig. 1). Genes were identified as cell cycle promoting or arresting on the basis of the previously reported function of each gene. Primer design was carried out using Primer3 and validated against reference RNA (Clontech, Mountain View CA, http://www.clontech.com). Total RNA was collected from primary cells using Trizol (Invitrogen), and cDNA was generated using Superscript III first-strand synthesis kits (Invitrogen) using oligo(dT) primers. Semiquantitative PCR was performed with variable template concentrations and PCR cycles to generate a linear range of amplification for each

gene. Individual band intensity was measured using ImageJ for a total of three independent experiments and expressed as mean ± SEM.

Western Blot Analysis

From each developmental period, 10^5 cells were lysed in a modified RIPA buffer containing the following: 150 mM NaCl, 50 mM EDTA (pH 7.5), 50 mM sodium β-glycerophosphate, 50 mM NaF, 5 mM sodium pyrophosphate, 2 mM EDTA, 2 mM EGTA, 1 mM dithiothreitol, 1 mM phenylmethylsulfonyl fluoride, 1 mM sodium orthovanadate with 1% Triton X-100, 10 μg/ml leupeptin, and 10 μg/ml aprotinin (Sigma-Aldrich). Equal amounts of lysates were resolved on a 12% SDS-polyacrylamide gel and transferred to a nitrocellulose membrane. The membrane was blocked in TBST (20 mM Tris-HCl [pH 7.5], 500 mM sodium chloride, and 0.05% Tween-20) containing 5% nonfat dry milk for 2 hours and then incubated with primary antibodies in TBST containing 1% bovine serum albumin at room temperature for 2 hours. Primary antibodies were as follows: cyclin A (rabbit α human, 1:200; Santa Cruz Biotechnology Inc., Santa Cruz, CA, http://www.scbt.com), cyclin D1 (mouse α human, 1:2,000; Santa Cruz Biotechnology), and cyclin E (rabbit α human, 1:200; Santa Cruz Biotechnology). Horseradish peroxidase-labeled secondary antibodies were applied in TBST containing 5% nonfat dry milk for 2 hours. Secondary antibodies were as follows: donkey α rabbit (1:10,000; Amersham Biosciences, Piscataway, NJ, http://www.amersham.com) and donkey α mouse (1:5,000; Amersham Biosciences). Protein was visualized by using an enhanced chemiluminescence detection system (Amersham Biosciences). ImageJ (NIH) was used to quantitate band intensity.

Fluorescence-Activated Cell Sorting Analysis

Triplicate populations from described developmental periods were trypsinized and collected as described. Pelleted cells were resuspended in 0.9% NaCl and were fixed with ice-cold ethanol. Fixed cells were pelleted and stored at 4°C for up to 3 days. Prior to analysis, cells for each condition were resuspended in PBS containing 50 μg/ml propidium iodide and 0.1 mg/ml RNase A for 30 minutes. Cells were analyzed for ploidy and cell cycle analysis using a FACScan flow cytometer (BD Biosciences, San Jose, CA, http://www.bdbiosciences.com), and data analysis was performed using Cell Quest data analysis software (BD Biosciences).

Immunocytochemistry

Cells plated on coverslips coated with poly-L-lysine or laminin and polyornithine (collectively LPO) were fixed with 4% paraformaldehyde (15 minutes, 25°C; Sigma-Aldrich). After being washed with PBS, cells were blocked for 20 minutes (attached cells) in PBS containing 10% FCS, 5% normal goat serum (Sigma-Aldrich), and 0.01% Triton X-100 (Sigma-Aldrich). Primary antibodies were applied for either 1 hour at 25°C or overnight at 4°C in PBS containing 10% FCS and 0.01% Triton X-100. Primary antibodies were as follows: A2B5 (recombinant A2B5-105; 1:500; Chemicon, Temecula, CA, http://www.chemicon.com), β-III-tubulin/Tuj1 (mouse monoclonal, 1:300, Promega, Madison, WI, http://www.promega.com; rabbit polyclonal, 1:500, Covance, Princeton, NJ, http://www.covance.com), BrDU (mouse monoclonal; 1:50; BD Biosciences), CD11b (rat monoclonal; 1:500; Chemicon), CD15 (mouse monoclonal; 1:300; Abcam, Cambridge, MA,

http://www.abcam.com), CD133 (rabbit polyclonal; 1:600; Abcam), CNPase (mouse monoclonal; 1:250; Chemicon), fibroblast growth factor receptor 1 (rabbit polyclonal; 1:500; GeneTex, San Antonio, TX, http://www.genetex.com), glial fibrillary acidic protein (GFAP; rabbit polyclonal; 1:600; Dako, Carpinteria, CA, http://www.dako.com), GFP (rabbit polyclonal; 1:300; Chemicon), Ki-67 (mouse monoclonal; 1:300; BD Biosciences), map2a-c (chicken polyclonal; 1:30,000; gift from Dr. Gerry Shaw), nestin (mouse monoclonal; 1:50; Chemicon), NeuN (mouse monoclonal; 1:500; Chemicon), NG2 (rabbit polyclonal; 1:500; Chemicon), O4 (mouse monoclonal IgM, 1:150; Chemicon), PSA-NCAM (mouse monoclonal; 1:500, Abcam), Sox1 (chicken polyclonal; 1:300; Chemicon), Sox2 (goat polyclonal; 1:500; R&D Systems), and Sox3 (rabbit polyclonal; 1:300; Chemicon). Secondary antibodies were applied for 1 hour at 25°C in PBS containing 10% FCS and 0.01% Triton X-100. Secondary antibodies were as follows: Alexa 555 goat α chicken (1:300; Molecular Probes, Carlsbad, CA, http://probes.invitrogen.com), Cy3 goat α mouse IgG (1:300; Jackson Immunoresearch Laboratories, West Grove, PA, http://www.jacksonimmuno.com), Cy3 goat α mouse IgM (1:600; Jackson Immunoresearch Laboratories), and Oregon Green goat α rabbit (1:600; Molecular Probes). For BrDU imaging, cells were incubated in sodium chloride/sodium citrate (SSC)-for-mamide (1:1, 37°C, 2 hours), washed three times for 10 minutes each in SSC, incubated in 2 N HCl (37°C, 30 minutes), and washed with 0.1 M borate buffer (25°C, 10 minutes). Nuclei were stained by application of either 4,6-diamidino-2-phenylindole (1 μg/ml, 25°C, 10 minutes; Sigma-Aldrich) or propidium iodide (50 μg/ml, 25°C, 10 minutes; Sigma-Aldrich) prior to mounting. For lipophilic dye addition, adherent cells were placed in ice-cold Hanks' balanced salt solution containing 5 μg/ml FM-143 (Molecular Probes) for 1 minute. Stained cells were mounted and immediately examined. Fluorescence microscopy and unbiased stereology were performed on a Leica DMLB upright microscope (Leica, Bannockburn, IL, http://www.leica.com), and images were captured with a Spot RT color charge-coupled device (CCD) camera (Diagnostic Instruments). Confocal microscopy was performed on an Olympus IX-70 microscope (Olympus, Melville, NY, http://www.olympus-global.com) using Confocal 1024 ES software (Bio-Rad, Hercules, CA, http://www.bio-rad.com). Unbiased stereology data were generated from three independent experiments, with each trial comprising a minimum of 12 visual fields at ×40 magnification. All valued were expressed mean ± SEM. Significance was determined by ANOVA or Student's *t* test.

Electron Microscopy

Passage 3 SVZ cells were grown in defined proliferative medium on LPO-coated aclar coverslips. Fixation and processing of thin sections was standard. Samples were visualized on a Leica EM10A transmission electron microscope at magnifications between ×1 and ×16,000. Images were captured using a CCD digital camera (Finger Lakes Instrumentation, Lima, NY, http://www.flicamera.com).

Neurosphere Formation and Clonal Fate Choice Assays

Subventricular progenitors were isolated from proliferating cells, and cells induced to differentiate for 1, 4, and 7 days were evaluated for neurosphere formation as described [1]. Briefly, cells were seeded in antiadhesive conditions at a density of 5×10^4 cells per milliliter in proliferative medium containing 1% methylcellulose (to increase medium

viscosity and decrease cellular aggregation). EGF and bFGF were supplemented every 2 days, and neurosphere formation was visually tracked using light microscopy at 7, 14, and 21 days. To measure multipotentiality, neurospheres were attached to LPO-coated coverslips and induced to differentiate as described and evaluated 3 days later. Positive control coverslips were selected proliferating cultures and proliferated in defined proliferative medium, resulting in no formation of neuroblasts.

Results

Differentiating Subventricular Astrocytes Transiently Adopt Tumorigenic Traits

To examine the normal differentiation of subventricular NSCs into committed cell types, we used a previously characterized cell culture model for the culture and differentiation of subventricular astrocytes [19]. Initial characterization of passage 1 SVZ-derived tissues revealed a heterologous cellular composition, including PSA-NCAM$^+$ and NeuN$^+$ neuronal cell types, CNPase$^+$ oligodendroglial cells, GFAP$^+$ astroglial cells, and CD11b$^+$ microglial cells (data not shown). Following culture in defined proliferative medium for three population doublings (~7–10 days), neuronal and oligodendroglial cell types (as distinguished by morphology and immunocytochemistry) were not observed. The primary proliferating population at this point is a heterogeneous mixture of cells displaying multiple primordial markers, including nestin and A2B5, and glial markers, including GFAP and vimentin [19] (data not shown). Microglial cell types were still detectable as a minor (<2% of total cell number) population and remained relatively constant throughout culture.

The removal of mitogenic stimuli has been reported as essential for generating committed progeny from NSCs [19, 31]. To examine the responses of neurogenic and non-neurogenic cells to mitogenic starvation, we compared the effects of growth factor withdrawal on total cell number and thymidine analog incorporation in subventricular- and cerebellar-derived tissues. Withdrawal of mitogenic stimuli in cerebellar cells resulted in decreases in total cell number (Fig. 1A) and thymidine analog incorporation (Fig. 1B). However, deprivation in subventricular-derived cells prompted increases in total cell number and thymidine analog incorporation (Fig. 1A, 1B).

Increased mitosis in SVZ tissues (in this case, signaling entry into terminal differentiation) is particularly curious considering that the prompting event is a removal of mitogenic stimuli. Normal somatic cells are generally dependent on consistent mitogen delivery for continued proliferation. This may represent entry into an aberrant or atypical growth state. As a loss of mitogenic dependence can represent the onset of neoplastic behaviors, we examined these cells for additional alterations in cell cycle during the generation of committed progeny. To accomplish this, we evaluated differentiation using semiquantitative PCR for a broad range of cell cycle genes (supporting information Fig. 1). Zero to 48 hours after mitogenic withdrawal to induce differentiation, subventricular cells upregulate proliferation-promoting genes (Fig. 1C), followed by their downregulation and upregulation of antiproliferative elements, beginning at 36 hours and generally subsiding 72 hours following initiation of differentiation (Fig. 1C, 1D). To confirm the coupling transcriptional and translational expression in this system, we compared the expression of cyclins A, D1, and E1 using semiquantitative Western blot (supporting information Fig. 2a); these cyclins exhibited

analogous alterations in protein expression levels. To gain further perspective on the dynamics of cellular proliferation accompanying differentiation, we treated subventricular and cerebellar cells at various stages following mitogenic withdrawal with propidium iodide and examined cell ploidy and cell cycle via fluorescence-activated cell sorting analysis. An elevated ratio of G1/2 to S-phase (suggesting a dramatic intracellular response) was appreciated shortly (12–24 hours) following the initiation of differentiation in SVZ-derived cultures (Fig. 1E), accompanied by an increase in the frequency of aneuploid cells in culture (Fig. 1F). These increases were not appreciated in identically cultured cerebellar-derived tissues. There was only a nominal increase in the total fraction of cells in S-phase during early differentiation (supporting information Fig. 2b), suggesting a modest generation of progenitor cells that subsequently proliferate dramatically. Increases in both G1/2 phase and aneuploidy in SVZ-derived tissue were attenuated with the subsequent appearance of stably diploid committed cell types (generally neurons). Forward scatter analysis revealed the enriched G1/2 population immediately following mitogenic withdrawal to be largely hyperploidic (data not shown). These findings indicated that although alterations in gene expression and cell cycle occur in the otherwise unremarkable generation of committed progeny, these aberrations are constrained to developmental states enriched for intermediate progenitors.

Interestingly, periods of alteration in proliferation, ploidy, and the molecular regulators of cell cycle all appear transient for progenitor-rich developmental states. One possibility for this is that the complex and heterologous cellular environment of our culture system may self-regulate abnormally proliferative and/or (proto)tumorigenic cells. This theory is supported by an upregulation of cell cycle arrest genes, most notably p53, following the generation of committed progeny (Fig. 1D). Since tumors tend to retain properties of their originating cells, freeing cells from this environment may allow better prospective identification of tumor-forming populations. In particular, we were interested in whether intermediate neural progenitors retain the intrinsic proliferative and multilineage potential retained in astrocytic gliomas. To test this hypothesis, we compared isolated cells from undifferentiated (NSC-enriched) SVZ to those differentiated for 1 day (progenitor-enriched), 4 days (enriched for early-stage committed progeny), or 7 days (enriched for late-stage committed progeny). Cells were trypsinized and seeded into antiadhesive conditions at clonal density for challenge in a neurosphere assay. Isolates from undifferentiated progenitor-rich populations formed equivalent numbers of neurospheres, whereas cells derived from more differentiated cells were progressively less able to generate primary neurospheres (Fig. 2A). To assess whether this generation of neurospheres is transient or sustainable, primary neurospheres were dissociated into secondary neurospheres. Although sphere-forming cells derived from other developmental time points generate secondary neurospheres at lower frequencies, primary neurospheres derived from progenitor-enriched time points were able to generate relatively higher percentages of secondary neurospheres (Fig. 2A), suggesting retention of proliferative index in the absence of a complex cellular microenvironment. Secondary spheres generated equivalent numbers of tertiary neurospheres, irrespective of initial developmental age of the originating sphere-forming cell or initial frequency of neurospheres generation (Fig. 2B). To further quantify the intrinsic proliferative capacity and developmental fate courses of cells generated under these

conditions, individual cells were selected as previously described and plated into adherent conditions favoring their differentiation. Individual clones were evaluated for proliferative capacity and fate of progeny 3 days later. Whereas cells derived from all stages of differentiation were able to generate all major neural lineages, clones derived from progenitor-rich developmental periods generated significantly larger numbers of $Tuj1^+$ neuroblasts than more or less differentiated cells (Fig. 2C). Whereas both isolates from both NSCs and their progenitors exhibited multilineage potential, clones derived from undifferentiated NSCs were largely quiescent and exhibited nominal self-renewal in conditions favoring their propagation (Fig. 2D). Cells derived from developmental periods enriched for committed progeny were able to generate similar numbers of committed neuroblasts but displayed diminished proliferative potential (Fig. 2C, 2D). These findings suggest that an unprecedented intrinsic proliferative index and multilineage potential are retained in developmentally intermediate progenitor cells.

Class III β-Tubulin Labels a Population of Transiently Tumorigenic Progenitor Cells

To prospectively identify potentially tumorigenic cells, we examined SVZ-derived cultures before, during, and after specification of committed cell types. Naïve and differentiating cells were longitudinally examined at 12-hour intervals using light microscopy and immunocytochemical labeling until the appearance of defined clusters of $PSA\text{-}NCAM^+$ neuroblasts 72–96 hours later. As class III β-tubulin frequently serves as a marker for astrogliomas, we examined differentiating cultures for atypical expression of this marker. After three population doublings in culture, undifferentiated SVZ cells occasionally weakly displayed the class III β-tubulin, often in cells displaying a protoplasmic astrocyte morphology with frequent coexpression of immature/stem markers. In these undifferentiated cells, class III β-tubulin labeled cells retaining protoplasmic morphology that typically extend one or more processes to contact adjacent cell bodies (Fig. 3A). Twelve to 24 hours following induction of terminal differentiation there was a strong upregulation of class III β-tubulin in a subpopulation of cells, generally constrained to two distinct cell types present in culture: a less prevalent hybrid cell type (Fig. 3B, left panel) that is morphologically similar to previously described intermediate cells, with morphology intermediate to astrocyte and neuron [32], and single cells containing scant cytoplasm and a retracted morphology (Fig. 3B, right panel). This expression of class III β-tubulin occurred unusually early for labeling emerging neurons and corresponded to a developmental period enriched for intermediate neural progenitors. Both intermediate and compacted cells coexpressed nestin, whereas GFAP was occasionally expressed only in the former. Whereas cells displaying an intermediate phenotype were present only transiently and in low number, compacted class $III\text{-}\beta\text{-}tubulin^+$ cells rapidly expanded in number and formed morphologically distinct clusters of densely packed cells (Fig. 3C, 3D, 3G). Class III $\beta\text{-}tubulin^+$ cells making up these clusters expressed EGF receptor (Fig. 3C, inset), matching a report for the expression of this receptor in developmentally intermediate cells [33]. Presumably, multinucleated cellular syncitiums are occasionally present within these clusters but are eventually supplanted by discrete individual cell bodies (as indicated by live cell labeling with lipophilic fluorophore-conjugated dye; data not shown). Twelve to 36 hours after differentiation was initiated, cells exhibited a lack of growth contact inhibition and grew on top of one another. Ultra-structural examination (via electron microscopy) of individual cells within these clusters indicated

increases in both mitochondria and lysosomes, as well as increases in the Golgi and free ribosomes (data not shown), suggesting an increase in transcription/translation. A progressive reduction in average nuclear size also accompanied differentiation within these clusters (9.6 ± 0.2 μm prior to differentiation; 5.1 ± 0.17 μm 72 hours following differentiation). Clusters of self-adherent neuroblasts, which are PSA-NCAM$^+$, Tuj1$^+$, GFAP$^-$, and nestin$^+$, were generated 72–96 hours after induction of differentiation (Fig. 3E) and morphologically developed into predominantly mature neurons (Fig. 3F). Cells within these characteristic clusters remained mitotically active (indicated by continued Ki-67 expression, BrDU uptake, and nuclear cleavages; data not shown), displayed scant cytoplasm and reduced numbers of mitochondria, and progressively dissociated and ceased division as neuronal maturation occurred (Fig. 3E, 3F).

Class III β-tubulin functions as a structural component of newborn and mature neurons. To verify that this marker is not merely activated extraordinarily early during in vitro or is an artifact of nonspecific labeling, we examined naïve cultures for the presence of class III β-tubulin using both mono- and polyclonal antibodies for class III β-tubulin/Tuj1. Interestingly, class III β-tubulin (albeit often in low levels) frequently colabeled with many of the consensus markers for immature cell types (Fig. 4A–4G), suggesting that it may be a useful tool for identifying primordial cells contributing to neurogenesis. Class III β-tubulin was also detectable in vivo in the subventricular wall of adult mice (Fig. 3H). Finally, reverse transcription-PCR for class III β-tubulin mRNA confirmed expression in all stages of subventricular NSC culture and differentiation (data not shown).

To correlate the previously described alterations in proliferative index and the subsequently arising aneuploidy, mitogenic insensitivity, and associated genetic dysregulation, we sought to determine whether class III β-tubulin labels the major population responding specifically to induction of differentiation. To achieve this, we measured class III β-tubulin$^+$ cells for the expression of Ki-67, a cell cycle marker that labels only proliferative cells. In SVZ-derived cultures, class III β-tubulin$^+$ cells were enriched for Ki-67 expression after 1 day of differentiation (supporting information Fig. 3a). Immunocytochemical detection indicated colocalization of Ki-67 and class III β-tubulin in cells located within the multicellular aggregations characterizing the progenitor → neuron specification (supporting information Fig. 3b). BrDU pulse labeling 12–36 hours postdifferentiation combined with labeling for class III β-tubulin revealed a majority (>85%) of class III β-tubulin$^+$ cells as being BrDU$^+$. Similarly assayed cerebellar cells exhibited heterologous class III β-tubulin expression but did not significantly coexpress primordial stem cell markers (data not shown). These findings suggest that in addition to identifying a major fraction of primordial cells, class III β-tubulin labels progenitors that actively participate in neurogenesis and likely retain previously characterized tumorigenic attributes.

Discussion

Using an adherent model for studying inducible organotypic neurogenesis, we define a unique approach for identifying potentially oncogenic cells within the developmental continuum bridging the astrocytic NSCs and their committed progeny. Primary neural stem cell populations react paradoxically to mitogenic withdrawal. Instead of entering a state of

cellular torpor (as is appreciated in non-neurogenic tissue), subventricular neural stem cells enter a state of increased proliferation characterized by increased aneuploidy, alterations in key cell cycle regulatory genes, and lack of growth contact inhibition. Study of these phenomena suggests that progenitors, rather than neural stem cells, may be more likely to form tumors in vivo. First, the development of hallmark cancerous traits is largely constrained to progenitor-enriched developmental periods, emerging after the initiation of differentiation and subsiding with the generation of defined progeny. Alterations in progenitors appear similar to the genetic aberrations appreciated in neural tumors [34], making progenitor populations a transient but unstable population. The notion of "transient instability" occurring in normal development is supported by several additional studies that document aberrations in chromosome numbers accompanying differentiation in vivo [35, 36]. Taken together, this evidence suggests that progenitors, rather than neural stem cells, comprise populations likely to yield astrocyte-derived tumors.

Conclusion

On the basis of the appreciated similarities to astrocytic gliomas, we hypothesize that neural progenitor populations comprise a pool of pretumorous cells that, if locked in this state, have a heightened capacity for tumor formation. In primary cultures, the increased expression of cell cycle arresting markers, combined with the failure to generate permanently transformed cells, suggests the possibility that external regulation may play a role in limiting neurogenic cells. Such regulation has already been appreciated [37]. To examine the intrinsic potential of neurogenic cells, we examined undifferentiated, differentiating, and fully differentiated cells for the ability to (a) proliferate and (b) yield multilineage progeny via the neurosphere assay. We found that progenitor cell-enriched developmental states displayed increased proliferative potential and retained multilineage potential in the absence of external cell-based input. This is significant, as multilineage-generating, highly proliferative gliomas are believed to closely resemble their originating cellular population.

Unlike previous studies, which have established links between NSCs and glioblastomas [2–6], our findings suggest that such tumors arise specifically from progenitor-rich periods. A number of observations support this argument. First, neurogenesis and tumorigenesis possess shared properties [38], suggesting that a cell type involved in this generation of committed progeny is essential as a tumor-originating cell. Second, adult neurogenesis proceeds from a relatively quiescent NSC described as glial in origin [13, 39, 40], which lacks properties associated with aggressive neural tumors. Third, compared with less differentiated NSCs or more differentiated neuronal progeny, progenitor cells retain a higher proliferative index and demonstrate multilineage potential, both characteristics that are observed in astrocytic tumors in vivo.

We next sought to identify individual cell types contributing to the observed pathologies. As the expression of class III β-tubulin is a conserved marker in astrocytic gliomas, we examined differentiating cells for aberrant expression of this marker in an attempt to proactively identify proto-oncogenic cells. Both naïve NSCs and differentiating progenitors heterologously expressed class III β-tubulin expression, whose expression colocalized with a variety of primordial NSC markers in undifferentiated cells and labels two discrete cell types

at the progenitor state. Following initiation of differentiation, class III β-tubulin$^+$ cells exhibited elevated expression of Ki-67 and BrDU incorporation, suggesting that these cells are a primary population (i.e., progenitors) involved in the generation of committed progeny. Interestingly, class III β-tubulin$^+$ cells express the receptor for EGF, a marker that is altered in a majority of human gliomas [41] and for which in vivo bombardment of the paired lateral ventricles with EGF results in the formation of tumor-like structures in ventricular tissue [16, 42]. As the proliferative response in class III β-tubulin$^+$ cells was unique to cells derived from the SVZ, we concluded that these cells are NSC-derived in origin. The precise role of class III β-tubulin$^+$ cells, including precise genetic and molecular alterations contributing to sustained tumorigenicity, should prove invaluable to unraveling the mechanisms through which astrocytic gliomas manifest. There is strong evidence that an aberrant class III β-tubulin expression seems to be associated with a variety of neural and non-neural tumors [20 –30], and the findings presented here on expression of this cytoskeletal protein in proliferative SVZ-derived cells provide additional evidence for associating these cells with the uncontrolled growth of neural progenitor cells and gliomagenesis. Although adult knockouts of class III β-tubulin have proved challenging to develop, the recent emergence of such models [43] provides promising opportunities for future functional studies.

Supplementary Material

Refer to Web version on PubMed Central for supplementary material.

Acknowledgments

Supported by NIH Grants NS055165, NS37556, HL70143 and the McKnight Brain Institute (to D.A.S.), NIH Grant NS46384 (to B.S.), and NIH Training Grant T32HD043730 (to N.M.W.). B.S. is supported by the Lichtenberg Program of the VW Foundation.

References

1. Kukekov VG, Laywell ED, Suslov O, et al. Multipotent stem/progenitor cells with similar properties arise from two neurogenic regions of adult human brain. Exp Neurol. 1999; 156:333–344. [PubMed: 10328940]
2. Ignatova TN, Kukekov VG, Laywell ED, et al. Human cortical glial tumors contain neural stem-like cells expressing astroglial and neuronal markers in vitro. Glia. 2002; 39:193–206. [PubMed: 12203386]
3. Hemmati HD, Nakano I, Lazareff JA, et al. Cancerous stem cells can arise from pediatric brain tumors. Proc Natl Acad Sci USA. 2003; 100:15178–15183. [PubMed: 14645703]
4. Galli R, Binda E, Orfanelli U, et al. Isolation and characterization of tumorigenic, stem-like neural precursors from human glioblastoma. Cancer Res. 2004; 64:7011–7021. [PubMed: 15466194]
5. Singh SK, Hawkins C, Clarke ID, et al. Identification of human brain tumour initiating cells. Nature. 2004; 432:396–401. [PubMed: 15549107]
6. Vescovi AL, Galli R, Reynolds BA. Brain tumour stem cells. Nat Rev Cancer. 2006; 6:425–436. [PubMed: 16723989]
7. Reya T, Morrison SJ, Clarke MF, et al. Stem cells, cancer, and cancer stem cells. Nature. 2001; 414:105–111. [PubMed: 11689955]
8. Passegué EJC, Ailles LE, Weissman IL. Normal and leukemic hematopoiesis: Are leukemias a stem cell disorder or a reacquisition of stem cell characteristics? Proc Natl Acad Sci U S A. 2003; 100:11842–11849. [PubMed: 14504387]

9. Uhrbom L, Dai C, Celestino JC, et al. Ink4a-Arf loss cooperates with KRas activation in astrocytes and neural progenitors to generate glioblastomas of various morphologies depending on activated Akt. Cancer Res. 2002; 62:5551–5558. [PubMed: 12359767]
10. Quiñones-Hinojosa A, Chaichana K. The human subventricular zone: A source of new cells and a potential source of brain tumors. Exp Neurol. 2007; 205:313–324. [PubMed: 17459377]
11. Tropepe V, Craig CG, Morshead CM, et al. Transforming growth factor-alpha null and senescent mice show decreased neural progenitor cell proliferation in the forebrain subependyma. J Neurosci. 1997; 17:7850–7859. [PubMed: 9315905]
12. Doetsch F, Garcia-Verdugo JM, Alvarez-Buylla A. Cellular composition and three-dimensional organization of the subventricular germinal zone in the adult mammalian brain. J Neurosci. 1997; 17:5046–5061. [PubMed: 9185542]
13. Doetsch F, Caille I, Lim DA, et al. Subventricular zone astrocytes are neural stem cells in the adult mammalian brain. Cell. 1999; 97:703–716. [PubMed: 10380923]
14. Yuan X, Curtin J, Xiong Y, et al. Isolation of cancer stem cells from adult glioblastoma multiforme. Oncogene. 2004; 23:9392–9400. [PubMed: 15558011]
15. Morshead CM, Craig CG, van der Kooy D. In vivo clonal analyses reveal the properties of endogenous neural stem cell proliferation in the adult mammalian forebrain. Development. 1998; 125:2251–2261. [PubMed: 9584124]
16. Doetsch F, Petreanu L, Caille I, et al. EGF converts transit-amplifying neurogenic precursors in the adult brain into multipotent stem cells. Neuron. 2002; 36:1021–1034. [PubMed: 12495619]
17. Hanahan D, Weinberg RA. The hallmarks of cancer. Cell. 2000; 100:57–70. [PubMed: 10647931]
18. Nakano I, Kornblum HI. Brain tumor stem cells. Pediatr Res. 2006; 59:54R–58R.
19. Scheffler B, Walton NM, Lin DD, et al. Phenotypic and functional characterization of adult brain neuropoiesis. Proc Natl Acad Sci U S A. 2005; 102:9353–9358. [PubMed: 15961540]
20. Katsetos CD, Herman MM, Mork SJ. Class III beta-tubulin in human development and cancer. Cell Motil Cytoskeleton. 2003; 55:77–96. [PubMed: 12740870]
21. Katsetos CD, Legido A, Perentes E, et al. Class III beta-tubulin isotype: A key cytoskeletal protein at the crossroads of developmental neurobiology and tumor neuropathology. J Child Neurol. 2003; 18:851–866. [PubMed: 14736079]
22. Katsetos CD, Del Valle L, Geddes JF, et al. Aberrant localization of the neuronal class III beta-tubulin in astrocytomas. Arch Pathol Lab Med. 2001; 125:613–624. [PubMed: 11300931]
23. Hessler RB, Lopes MB, Frankfurter A, et al. Cytoskeletal immunohistochemistry of central neurocytomas. Am J Surg Pathol. 1992; 16:1031–1038. [PubMed: 1471723]
24. Hirose T, Scheithauer BW, Lopes MB, et al. Dysembryoplastic neuroeptihelial tumor (DNT): An immunohistochemical and ultrastructural study. J Neuropathol Exp Neurol. 1994; 53:184–195. [PubMed: 8120540]
25. Lopes MB, Altermatt HJ, Scheithauer BW, et al. Immunohistochemical characterization of subependymal giant cell astrocytomas. Acta Neuropathol. 1996; 91:368–375. [PubMed: 8928613]
26. Martinez-Diaz H, Kleinschmidt-DeMasters BK, Powell SZ, et al. Giant cell glioblastoma and pleomorphic xanthoastrocytoma show different immunohistochemical profiles for neuronal antigens and p53 but share reactivity for class III beta-tubulin. Arch Pathol Lab Med. 2003; 127:1187–1191. [PubMed: 12946225]
27. Woulfe J. Class III beta-tubulin immunoreactive intranuclear inclusions in human ependymomas and gangliogliomas. Acta Neuropathol. 2000; 100:427–434. [PubMed: 10985703]
28. Prasannan L, Misek DE, Hinderer R, et al. Identification of beta-tubulin isoforms as tumor antigens in neuroblastoma. Clin Cancer Res. 2000; 6:3949–3956. [PubMed: 11051243]
29. Katsetos CD, Kontogeorgos G, Geddes JF, et al. Differential distribution of the neuron-associated class III beta-tubulin in neuroendocrine lung tumors. Arch Pathol Lab Med. 2000; 124:535–544. [PubMed: 10747310]
30. Dozier JH, Hiser L, Davis JA, et al. Beta class II tubulin predominates in normal and tumor breast tissues. Breast Cancer Res. 2003; 5:R157–R169. [PubMed: 12927047]

31. Walton NM, Sutter BM, Chen HX, et al. Derivation and large-scale expansion of multipotent astroglial neural progenitors from adult human brain. Development. 2006; 133:3671–3681. [PubMed: 16914491]
32. Laywell ED, Kearns SM, Zheng T, et al. Neuron-to-astrocyte transition: Phenotypic fluidity and the formation of hybrid asterons in differentiating neurospheres. J Comp Neurol. 2005; 493:321–333. [PubMed: 16261530]
33. Sun Y, Goderie SK, Temple S. Asymmetric distribution of EGFR receptor during mitosis generates diverse CNS progenitor cells. Neuron. 2005; 45:873–886. [PubMed: 15797549]
34. Zhu Y, Parada LF. The molecular and genetic basis of neurological tumours. Nat Rev Cancer. 2002; 2:616–626. [PubMed: 12154354]
35. Kaushal D, Contos JJ, Treuner K, et al. Alteration of gene expression by chromosome loss in the postnatal mouse brain. J Neurosci. 2003; 23:5599–5606. [PubMed: 12843262]
36. Yang AH, Kaushal D, Rehen SK, et al. Chromosome segregation defects contribute to aneuploidy in normal neural progenitor cells. J Neurosci. 2003; 23:10454–10462. [PubMed: 14614104]
37. Walton NM, Sutter BM, Laywell ED, et al. Microglia instruct subventricular zone neurogenesis. Glia. 2006; 54:815–825. [PubMed: 16977605]
38. Phillips HS, Kharbanda S, Chen R, et al. Molecular subclasses of high-grade glioma predict prognosis, delineate a pattern of disease progression, and resemble stages in neurogenesis. Cancer Cell. 2006; 9:157–173. [PubMed: 16530701]
39. Laywell ED, Rakic P, Kukekov VG, et al. Identification of a multipotent astrocytic stem cell in the immature and adult mouse brain. Proc Natl Acad Sci U S A. 2000; 97:13883–13888. [PubMed: 11095732]
40. Imura T, Kornblum HI, Sofroniew MV. The predominant neural stem cell isolated from postnatal and adult forebrain but not early embryonic forebrain expresses GFAP. J Neurosci. 2003; 23:2824–2832. [PubMed: 12684469]
41. Mellinghoff IK, Wang MY, Vivanco I. Molecular determinants of the response of glioblastomas to EGFR kinase inhibitors. N Engl J Med. 2005; 353:2012–2024. [PubMed: 16282176]
42. Kuhn HG, Winkler J, Kempermann G, et al. Epidermal growth factor and fibroblast growth factor-2 have different effects on neural progenitors in the adult rat brain. J Neurosci. 1997; 17:5820–5829. [PubMed: 9221780]
43. Liu L, Geisert EE, Frankfurter A, et al. A transgenic mouse class-III beta tubulin reporter using yellow fluorescent protein. Genesis. 2007; 45:560–569. [PubMed: 17868115]

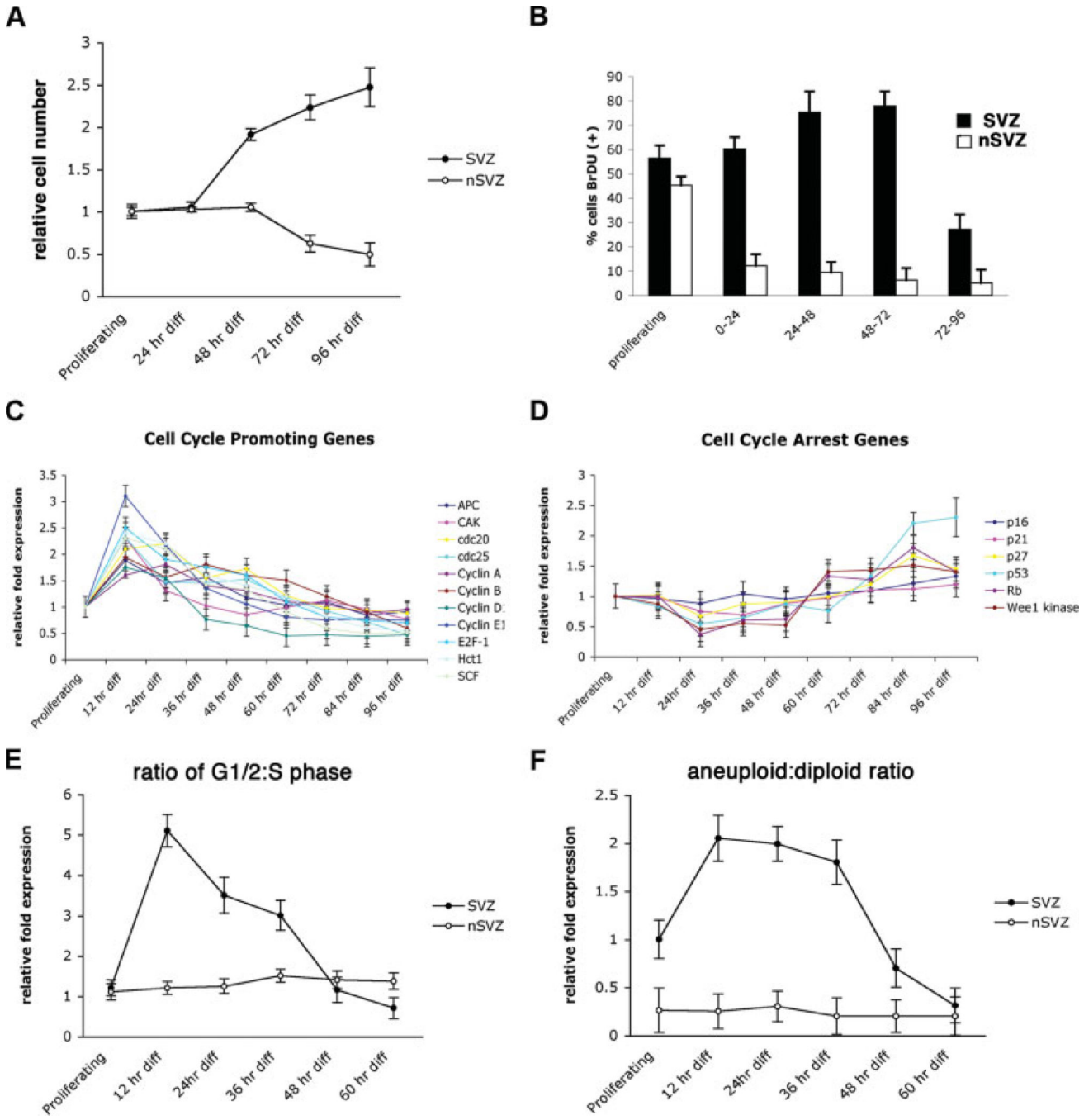

Figure 1.

Transient alterations in proliferation, ploidy, and gene regulation characterize subventricular differentiation. **(A):** Subventricular-derived NSCs proliferated in response to removal of mitogenic stimuli. **(B):** Twenty-four-hr incremental BrDU pulse labeling revealed increases in thymidine analog incorporation 24–72 hr following mitogenic differentiation in subventricular cultures. Alteration in gene expression accompanied differentiation in SVZ tissues: increases in cell cycle promoting genes 12–36 hr following mitogenic withdrawal **(C)** were followed by increases in cell cycle checkpoint genes **(D)**. Mitogenic deprivation

signaled increases in cellular growth **(E)** and aneuploidic (hyperploidic) cells **(F)**, which were resolved upon the generation of neuroblasts. Abbreviations: BrDU, 5′-bromodeoxyuridine; diff, differentiated; hr, hour; nSVZ, non-subventricular zone; SVZ, subventricular zone.

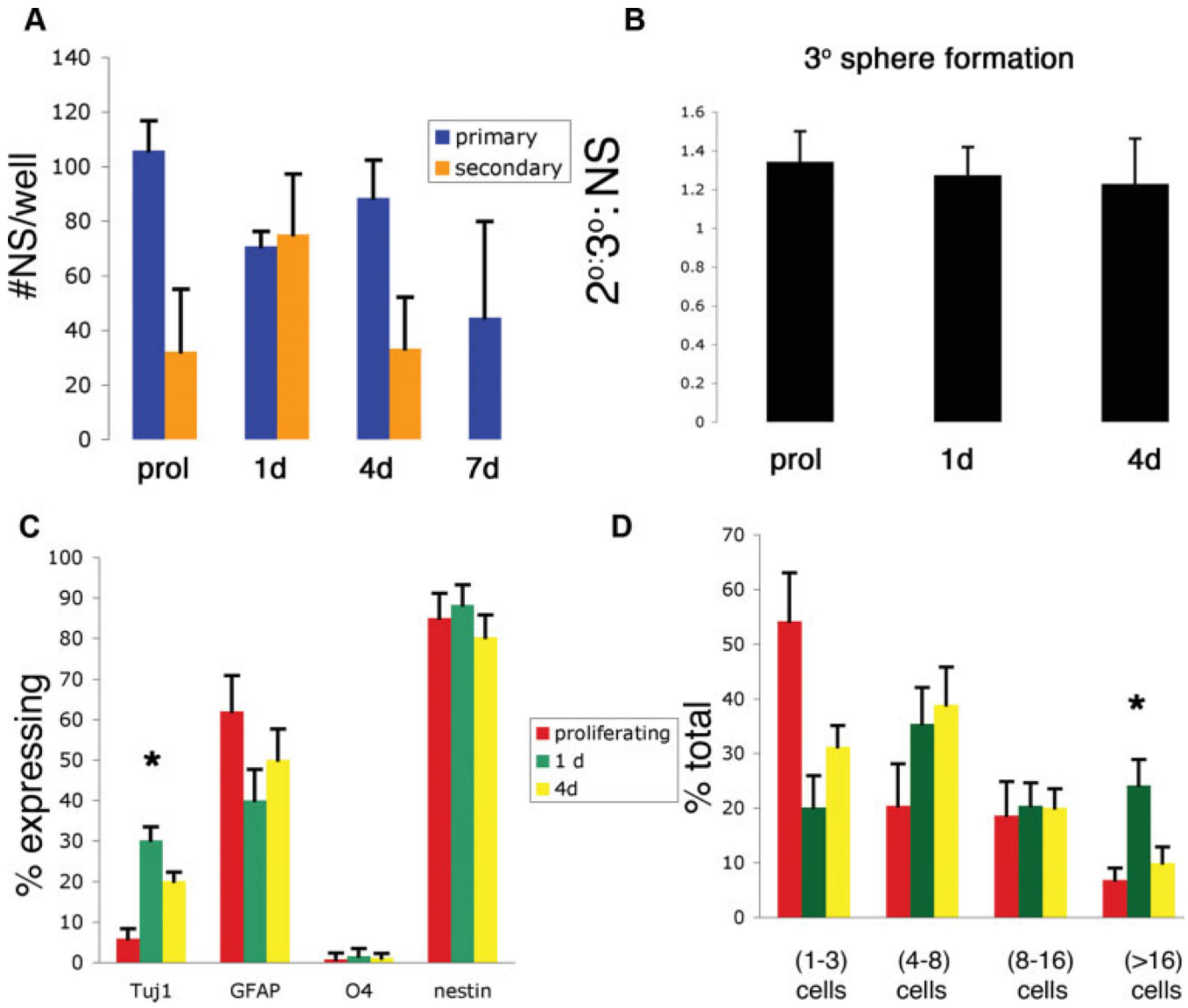

Figure 2.

The absence of a complex multicellular environment yield enhances proliferation and multilineage potential in neural progenitors. **(A):** Quantified NS production from prol and differentiating (1, 4, or 7 d) subventricular zone (SVZ)-derived NSCs. **(B):** 3° sphere formation from 2° spheres generated in **(A)**. **(C):** Progeny analysis of adherent individual cells expanded clonally for 3 d. **(D):** Proliferative capacity of individual SVZ cells placed in NS-forming conditions for 3 d. *, $p < .05$; one-way analysis of variance. Abbreviations: 2°, secondary; 3°, tertiary; d, day; GFAP, glial fibrillary acidic protein; NS, neurosphere; prol, proliferating.

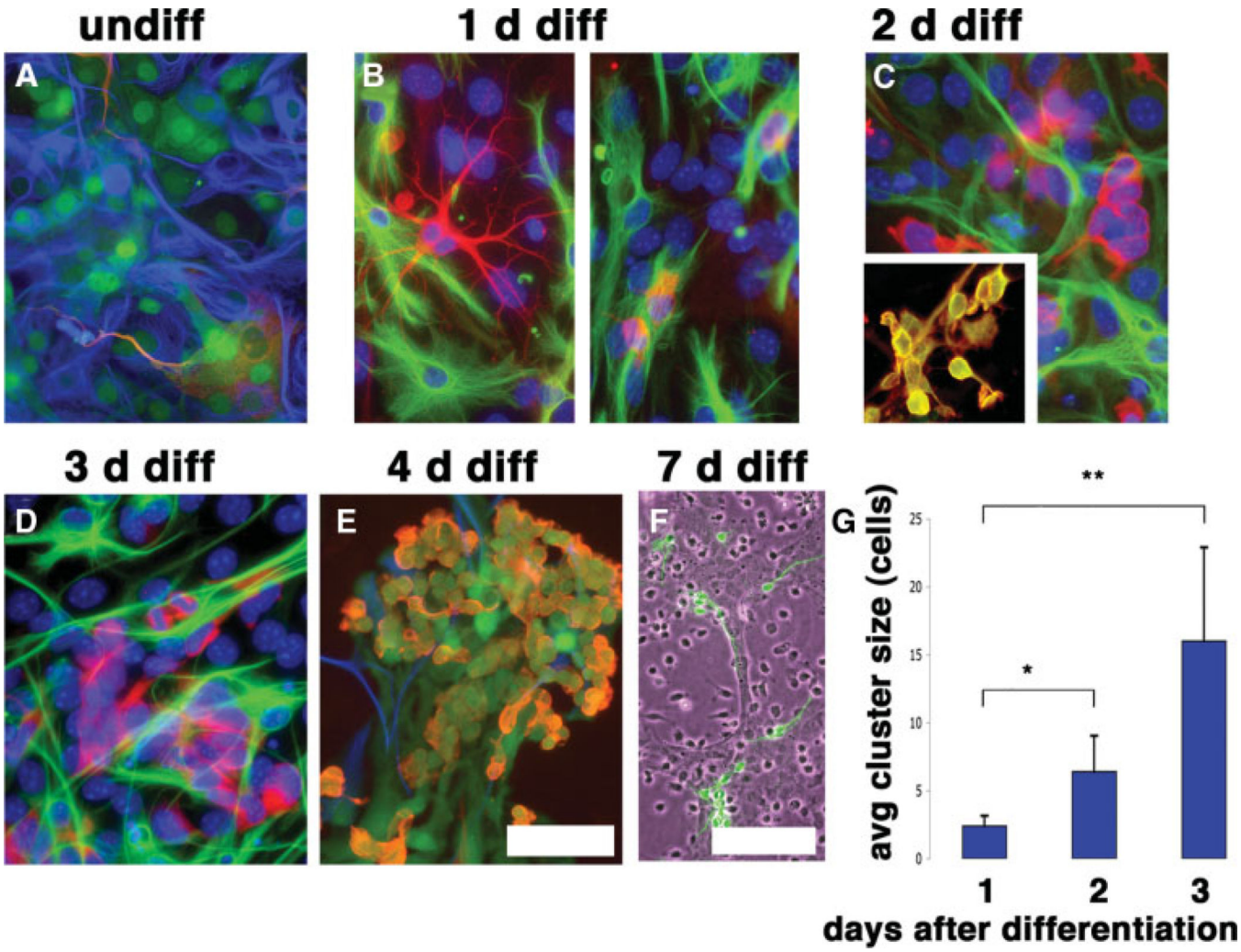

Figure 3.

Differentiation of astrotypic NSCs results in the upregulation of class III β-tubulin in intermediate progenitor cells. **(A):** Class III β-tubulin was appreciated in undiff cultures in cells generally possessing a protoplasmic astrocyte morphology (βIII-tubulin, red; glial fibrillary acidic protein [GFAP], blue; nestin-enhanced green fluorescent protein, green). **(B):** One d following induction of differentiation, compact single $GFAP^{-}$/class III β-$tubulin^{+}$ cells (left) were present, with a minor population of $GFAP^{+/-}$/class III β-$tubulin^{+}$ cells (right) with an indeterminate morphology. **(C):** Compacted progenitors multiplied to form clusters following their appearance in culture. Progenitors at this developmental stage expressed epidermal growth factor receptor (red, inset) (class III β-tubulin, green). **(D, E):** Progenitors matured to form clusters of neuroblasts, which appeared in culture 4 d following differentiation **(E)** and formed defined neuronal phenotypes (class III β-tubulin, green). **(G):** Class III β-$tubulin^{+}$ progenitors exhibited rapid expansion following their appearance in culture. Images show counterstaining with 4,6-diamidino-2-phenylindole. Scale bars = 50 μm **(A–E)**, 100 μm **(G)**. *, $p < .05$; **, $p < .05$; one-way analysis of variance. Abbreviations: avg, average; d, days; diff, differentiated; undiff, undifferentiated.

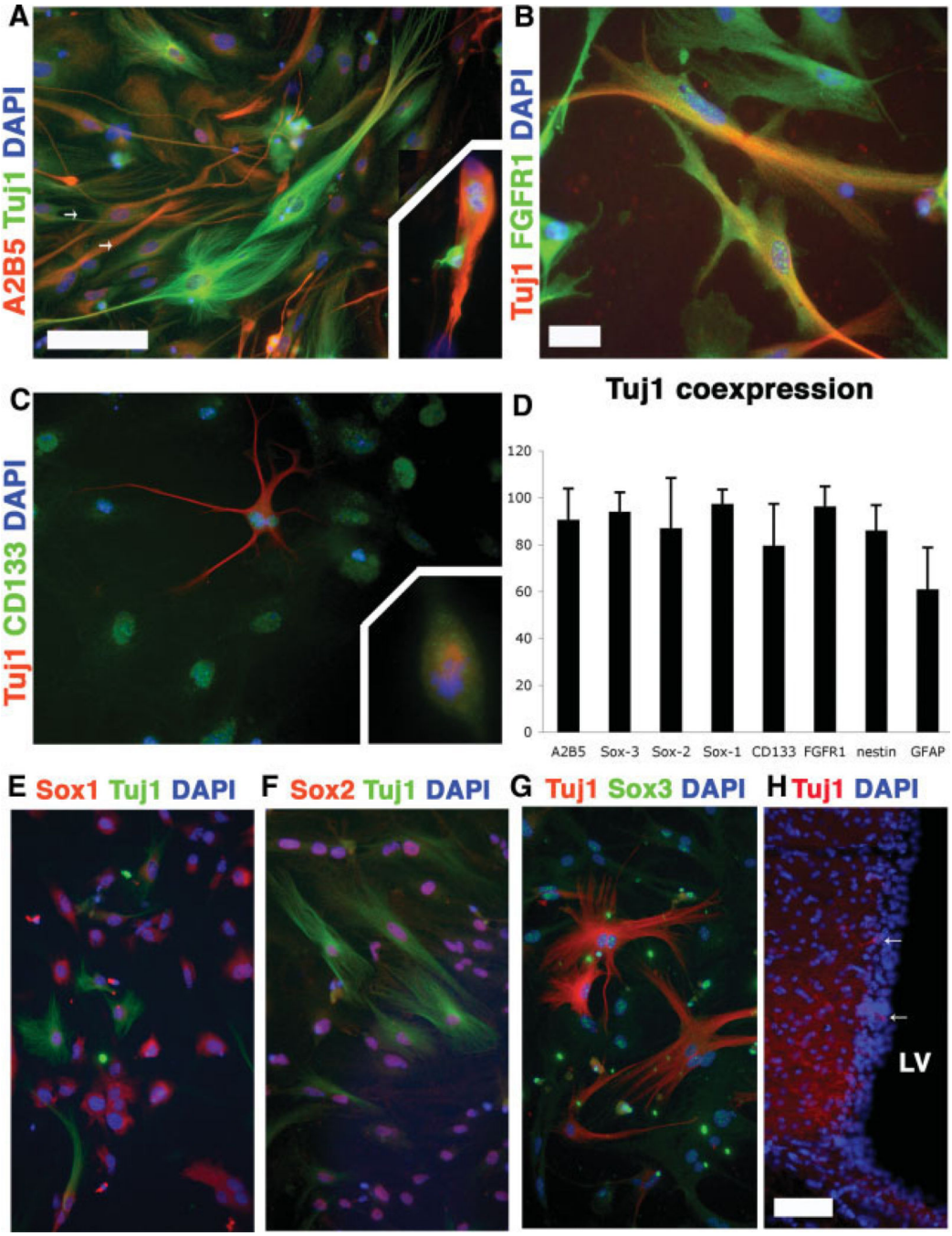

Figure 4.

Class III β-tubulin/Tuj1 labels putative neural stem cell (NSC)/progenitor populations. Multiple antibody labeling in undifferentiated passage 3 subventricular NSCs revealed coexpression of A2B5 (**[A]**, arrows), FGFR1 **(B)**, and CD133/Prominin-1 **(C)**. Tuj1 was expressed in the mitotic spindle of dividing cells (**[A, C]**, insets). **(D):** Substantial fractions of $Tuj1^{+}$ cells expressed NSC and progenitor markers. CD15 and NG2 were examined and were not expressed in undifferentiated cultures. **(E–G):** Tuj1 was expressed in multiple members of the Sox protein family, as well as in the supependymal cell layer of the lateral

ventrical (**H**). Coronal section of the subventricular zone revealed that Tuj1^{+} cells were present in the subventricular layer adjacent to the LV (arrows). Scale bars = 50 μm **(A, C, E–G)**, 25 μm **(B)**, and 100 μm **(H)**. Abbreviations: DAPI, 4,6-diamidino-2-phenylindole; FGFR1, fibroblast growth factor receptor 1; GFAP, glial fibrillary acidic protein; LV, lateral ventricle.